Probing the Surface Swelling in Ultra-Thin Supported Polystyrene Films During Case II Diffusion of n-Hexane

Wojciech Ogieglo, Herbert Wormeester, Matthias Wessling, Nieck E. Benes*

In situ time-resolved spectroscopic ellipsometry is used to study the dynamics of n-hexane diffusion into, and the corresponding induced swelling of, ultra-thin polystyrene films. The experimental conditions are carefully selected to facilitate the observation of anomalous Case II diffusion in the system, thereby allowing the probing of the chain-relaxation dynamics of a sharp moving penetrant front within the films. It has been found that the two different approaches to the obtained data are in quantitative agreement and suggest the existence of a finite thickness region of 14 ± 3 nm in the outer film interface that is instantly swollen after contact with the penetrant. The thickness of this fast swelling layer is found to be independent of swelling temperature and physical aging time. After the interface is swollen, the diffusion front velocity shows no significant spatial variations in the direction perpendicular to the substrate, but is strongly dependent on temperature and sample aging history.

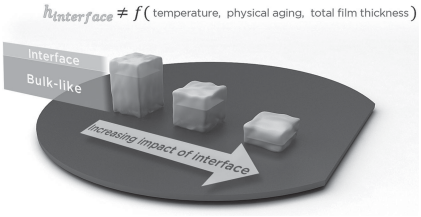

1. Introduction

Decreasing the thickness of polymer films below about 100 nm has been claimed to result in deviations of materials properties as compared with those of the bulk polymer. Such phenomena are commonly referred to as nano-confinement effects and are generally explained in terms of an increased contribution of interfaces to the behavior of ultra-thin films.[1–15] A typical result is a deviation of the glass transition temperature (T_g) of a thin film from the characteristic value of the bulk polymer. Although still a subject of an intense debate, the most common explanations for nano-confinement effects are different molecular mobility at the film interfaces, or a gradient of dynamics within the thin film. For polystyrene thin films, a reduction of T_g with decreasing thickness is generally reported. This is explained by the increasing contribution of the free film interface that possesses a higher segmental mobility than the bulk.[14,15] In the case of poly(methyl methacrylate) (PMMA), and other polymers with hydroxyl groups,[6,7,16,17] an increase in T_g with decreasing thickness of the film has been reported. The increase in T_g is explained in terms of the dominant contribution of an immobilized (or adsorbed) layer of polymer directly at the interface with the substrate. For PMMA, evidence of an increased mobility at the outer (free) interface has also been reported.[18]

On the other hand, Tress et al.[19] using a combination of broadband dielectric spectroscopy (BDS), ellipsometry, X-ray reflectometry (XRR), and alternating current (ACC) as well as differential scanning calorimetry (DSC) have shown no evidence of significant deviations of T_g from the bulk, for polystyrene layers down to about 5 nm,

W. Ogieglo
Membrane Science and Technology, Mesa+ Institute for Nanotechnology, University of Twente, P.O. Box 217 7500, AE Enschede, The Netherlands
Dr. H. Wormeester
Physics of Interfaces and Nanomaterials, Mesa+ Institute for Nanotechnology, University of Twente, P.O. Box 217 7500, AE Enschede, The Netherlands
Prof. M. Wessling
RWTH Aachen University, Chemical Process Engineering, Turmstrasse 46, 52064, Aachen, Germany
Dr. N. E. Benes
Inorganic Membranes, Mesa+ Institute for Nanotechnology, University of Twente, P.O. Box 217 7500, AE Enschede, The Netherlands
E-mail: n.e.benes@utwente.nl

DOI: 10.1002/macp.201300371

for a wide range of molecular weights. The same was found for PMMA down to 10 nm thickness in a study of Erber et al.[20] These authors suggested that the apparent deviations of T_g found by other researchers are related to sample preparation artifacts (annealing, removal of residual solvent etc).

There have been a few studies dedicated to the direct study of polymer surface dynamics. Most notably, Fakhraai and Forrest[9] have demonstrated, using a nanoparticle embedding technique, that the glassy polymer surface has an orders of magnitude higher mobility as compared with the bulk. In their experiments, they observed relaxation of nano-scale indentations (craters) left after removal of gold nanoparticles from the polymer surface. These relaxations occur relatively fast, even at temperatures as low as 100 K below the T_g, suggesting the existence of a liquid-like layer at the surface. Very convincing evidence of increased surface mobility have also been provided by the observations of dynamic rigid percolating solid fractal structures near T_g.[21,22] These time-resolved studies suggest that, even well below T_g, the surface is characterized by significant mobility that can be well described by the twinkling fractal theory. The thickness of the layer with increased mobility is estimated to be 0.1–10 nm.[23,24] This thickness is often larger than the length of the cooperatively rearranging region (CRR) at glass transition (1–3 nm),[25] and does not seem to significantly depend on the total film thickness.[26] The surface mobility layer is shown to be characterized by dynamics much faster than for the bulk polymer, with estimates reaching a factor of 10^9.[27] The increased surface dynamics have also been shown in other glassy systems, including small molecule glass formers.[28]

Apart from increased surface chain mobility, other explanations of nano-confinement effects have also been proposed. One of them is the reduced local entanglement density at the polymer interface, which has been suggested based on experiments involving thinning of suspended polymer fibers.[29] As suggested in that study, a threshold of film thickness exists at $h/R_{ee} < 2$ below which the entanglement density significantly decreases and self-entanglements become more significant. Related to that the viscosity of the polymer network at the interface was found to be orders of magnitude lower, leading to much higher deformability.[15,30–32]

Studies involving in situ experiments of swelling of thin and ultra-thin films in liquid penetrants are very rare, mainly due to the associated experimental difficulties.[18,33] In one investigation, Hori et al.[18] analyzed Case II diffusion of methanol in poly(methyl methacrylate) ultra-thin films, by an optical reflectivity method. They found an increase in diffusion coefficient of methanol at the free surface of the film substantiating the existence of a surface region with increased mobility. Below a certain threshold value of the total film thickness, also the influence of the immobilized substrate layer is noticeable. These mutual effects are shown to occur in a surprisingly large thickness range (below about 70–90 nm). In the study of Hori et al.,[18] the dynamics of Case II diffusion were shown to be a good measure of the polymer chain dynamics, allowing resolving possible spatial deviations in dynamics in the direction perpendicular to the substrate.

In the present study, in situ time-resolved spectroscopic ellipsometry has been applied to investigate surface properties of ultra-thin supported polystyrene films, during swelling with n-hexane. The conditions of the experiments have been carefully selected to force transport of n-hexane into the film to occur by Case II anomalous diffusion. This enables to probe spatial variations in the chain dynamics in the direction perpendicular to the substrate, as a function of sample history (aging) and temperature. The obtained data have been analyzed via two distinct methods. The first method is based on numerical fitting of a multi-layer optical model to the ellipsometry data and yields the time evolution of the thicknesses of a swollen part of the film and a non-swollen part. The second method is based on deriving kinetics of the diffusing front from changes in the raw Ψ and Δ data. Both approaches are shown to confirm the existence of an almost instantly swollen layer at the top interface and allow quantifying its thickness. The study presents evidence supporting a different behavior of the surface of a thin film than for bulk material, and its consequences for the diffusion of small molecule penetrants. Such processes are relevant in many thin film application areas, e.g., membranes, barriers, and coatings.

2. Theory

2.1. Anomalous Case II Diffusion

Case II diffusion occurs as a result of a difference between the diffusion timescales of a small molecule penetrant in the rubbery and glassy state of the polymer.[34,35] The diffusion coefficient in a rubbery state is 3–4 orders of magnitude larger than in the glassy state.[36] The consequence is that an anomalous, non-Fickian, mechanism of diffusion occurs in which the limiting process is polymer chain relaxation, not the Fickian diffusion of the penetrant. Case II diffusion is characterized by the migration of a sharp front that divides the film into a completely swollen region and an essentially dry region.[37,38] In the swollen region, the penetrant plasticizes the polymer severely and the system becomes a rubber; the dry part of the film still remains far below its T_g. Because of the large difference in penetrant mobility in the two regions, the process of diffusion is only limited by the chain relaxations at the glass

transition front. This enables to separate polymer chain relaxations, of interest in the studies presented here, from the diffusion process. The approach is valid for polystyrene films thinner than about 1–2 μm, where diffusion through the swollen outer layer can be considered infinitely fast and the process is manifested by a linear increase of film dilation (or weight) in time. Such behavior is found to occur at temperatures slightly above the penetrant induced T_g, which is about 20–22 °C for a polystyrene–n-hexane system.[39] Below that temperature, the swollen region of the film remains glassy and a sharp diffusion front does not develop. That process can be described by the Berens–Hopfenberg model,[40] because diffusion and relaxation occur on similar timescales. The linear dependence of swelling on time no longer holds and curves are obtained that are more characteristic for Fickian diffusion.

2.2. Spectroscopic Ellipsometry Principles and Data Analysis

Spectroscopic ellipsometry is based on the measurement of the change of polarization state of light reflected from a flat sample. Polarization states that are in-plane or out-of-plane of incidence, *p* and *s* respectively, are distinguished. The ratio of the reflectivity for these two polarizations is used, characterized by the ellipsometric parameters Ψ and Δ:

$$\rho = \frac{r_p}{r_s} = \tan(\psi)\exp i\Delta \quad (1)$$

The Ψ and Δ parameters measured across a broad spectral range form the ellipsometric spectra. Ψ and Δ can be converted into useful sample properties, such as film thickness and refractive index, by numerical fitting of an appropriate optical model to the ellipsometric spectra. For swelling of polymer samples, both of these film thickness and refractive index are associated with the penetrant uptake. However, since they are determined independently of each other (at least down to a thickness of about 25 nm), the volume dilation data (thickness change) can be, in principle, confronted with sample density changes (refractive index change).

The extraction of sample properties is done based on a numerical fitting of the model generated data to the experimentally obtained Ψ and Δ. As a goodness of fit, an *MSE* ((root) mean square error), parameter is used. This parameter is a measure of an error between the modeled and experimental spectrum. For samples thinner than about 100 nm, a good fit is considered to have an *MSE* of 1–2. For thicker films, larger *MSE* values are acceptable. For more details on the technique and optical modeling, the interested reader is referred to a spectroscopic ellipsometry handbook.[41,42] The advantage of this technique for in situ optical characterization is that the values of the measured parameters do not depend on the absolute light intensity, only on the polarization state. This implies that the technique is not very sensitive to, for instance, light attenuation by a fluid ambient.

Spectroscopic ellipsometry allows determining, independently, film thickness, and refractive index down to a film thickness of about 25 nm. For thinner films, the thickness and refractive index become highly correlated to each other. Despite the unfeasibility to separate thickness and refractive index, for very thin films changes in Ψ and Δ spectra can still be determined very accurately, allowing to study for instance the kinetics of transient processes and glass transitions.[43,44]

3. Experimental Section

3.1. Film Preparation and Sample Treatment

Thin films of polystyrene (T_g = 100.0 °C by DSC onset, $\overline{M}_w$ = 280 kg mol^{-1}; Sigma Aldrich) were spin-coated on silicon wafers from a toluene solvent (Merck). The thicknesses were adjusted by varying the solution concentration in the range from 0.8% to 3%. The rotational speed of the spin-coater platform was 2000 rpm and the coating was done on already rotating samples using about 0.5 mL of the polymer solution. The substrates were thoroughly cleaned with 3:1 (vol.) mixture of 98% sulfuric acid (Sigma–Aldrich) and 30% hydrogen peroxide (Sigma–Aldrich) to remove any organic impurities. Just before spin-coating, they were flushed with dry nitrogen to remove any dust or particles, which would cause film defects. After spin-coating, the samples were dried in air and transported to a nitrogen flushed oven set at 130 °C for annealing. After at least 3 h of annealing, the supported thin films were quenched to room temperature and left to physically age for 1 h or 2 weeks. The aging was done at room temperature (21 ± 1 °C).

3.2. Measurement Procedure

A spectroscopic ellipsometer (M-2000X, J. A. Woollam Co., Inc.) was used to track the swelling of ultra-thin polystyrene films. The data acquisition rate was about 2 s per full spectral scan and the spot size was about 2 mm. The in situ cell used was made of glass with windows positioned perpendicular to the probing light beam. The angle of incidence was fixed at 70° and the wavelength range used for fitting was from 340 to 1000 nm. Further details of the experimental setup can be found in ref. [45].

The aged samples (either for 1 h or for 2 weeks) were swollen with liquid n-hexane at two temperatures: 23 °C and 26 °C. For each experiment, a fresh sample was used. The measurement was always done according to the following experimental procedure. The aged sample was transported to the glass in situ cell after exactly 1 h or 2 weeks of aging time. First, the dry sample parameters (thickness, optical dispersion) were determined. Afterwards, thermally equilibrated liquid n-hexane was introduced to the cell and the measurement was started within a maximum of 45 s from that moment. This time was required to correct for minor sample misalignments, mechanical equilibration of the system, and setting up the time-resolved

data acquisition. The amount of time used was slightly different for each sample, therefore, it was carefully recorded and included in the kinetic data. The measurement was continued until no significant change in the raw data occurred (usually within 1.5 h from the start of the measurement).

Correction for the Δ offset in-plane of incidence was done using an appropriate fitting parameter based on the data for dry films. The parameter was then used as a non-fitting parameter in the n-hexane swelling experiments. The correction for the out-of-plane offset was automatically performed by the software of the ellipsometer utilizing the appropriate design of the instrument.

3.3. Data Analysis and Modeling

To extract properties of dry films and of equilibrium-swollen films (obtained at the end of kinetic experiments), an optical model of stacked layers was used. This model involved a silicon wafer support (with a thin native oxide layer taken into account), onto which a layer representing the polymer film was placed. The polymer layer was considered uniform and homogeneous and its optical dispersion was modeled with a two-term Cauchy relation:

$$n(\lambda) = A + \frac{B}{\lambda^2} \quad (2)$$

The film thickness and parameters A and B were fitted to the Ψ and Δ spectrum. Often a third parameter, C, is used to model the optical dispersion of polymeric films (contributing a term C/λ^4 to the dispersion). However, since already fitting of A and B resulted in sufficiently low *MSE* for all of the analyzed samples, and the decrease of the *MSE* by including C was limited, it was omitted in the optical dispersion to avoid overparametrization. The dispersion of n-hexane with an ellipsometric measurement on a well-characterized substrate (25 nm of thermal SiO_2 on Si) submerged in the fluid after equilibration at the desired temperature. This provided optical dispersion parameters of n-hexane: $A_{H,23\ °C}$ = 1.375, $B_{H,23\ °C}$ = 0.0008195 μm^2 and $C_{H,23\ °C}$ = 0.00044098 μm^4, and $A_{H,26\ °C}$ = 1.373, $B_{H,26\ °C}$ = 0.00073606 μm^2 and $C_{H,26\ °C}$ = 0.00044781 μm^4. The corresponding refractive index values at 632.8 nm were 1.380 and 1.378, respectively. These data are in a very good agreement with literature.[46]

For the tracking of the Case II wave progression, the layer representing the polymer film was separated in two parts as shown in Figure 1. As we showed previously,[45] the Case II process can be represented by two distinct layers, separated by a sharp interface (front). The properties of the layer that is in contact with the penetrant (swollen film) were assumed identical to those of the fully swollen films (typical refractive index at 632.8 nm of 1.562). The other layer, in contact with the support (remaining dry film), was considered non-swollen and to have properties identical to that of the dry film (typical refractive index at 632.8 nm of 1.585). With this approach, the fitting parameters for this model are limited to the thickness of the swollen layer and the thickness of the dry layer. In such a way, the progression of the Case II front could be tracked in time with a relatively high spatial resolution in the direction perpendicular to the substrate.[45] Simultaneous fitting of both the thicknesses and indices of swollen and dry layers has proven very unreliable due to high fit parameter correlations as a result of little optical

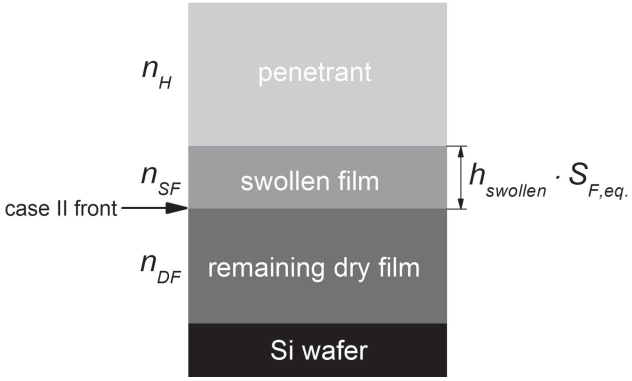

Figure 1. Two-layer optical model used to track the Case II mechanism of n-hexane swelling in ultra-thin, silicon wafer supported polystyrene films; n_H, n_{SF}, and n_{DF} stand for refractive indices (at 632.8 nm) of n-hexane, swollen and dry parts of the film respectively; $h_{swollen}$ represents thickness of the region of the film that has been swollen to a thickness $h_{swollen}S_{F,eq.}$

contrast between the layers (small Δn of 0.023), and the very small thickness of the swollen layer at the beginning of swelling (below 25 nm). The introduction of liquid n-hexane further reduced the optical contrast during the measurement ($n_H > n_{air}$). For the same reasons, accurate determination of possible smooth density gradients associated with the initial stages of diffusion has been considered not possible.

4. Results and Discussion

In polystyrene swollen by n-hexane, Case II diffusion occurs above the penetrant-induced glass transition (20–22 °C).[45] In the present study, experiments have been conducted at 23 °C and 26 °C. At 23 °C, the swollen film is only slightly above the glass transition, allowing the swelling to be tracked in a conveniently long experimental timescale. For instance, equilibrium is obtained after about 50 min for ≈100 nm samples. Close to the glass transition, the diffusion front is not very sharp but has a small, yet significant, finite thickness. As a consequence, the two-layer model, Figure 1, may be inaccurate. However, as seen in Figure 2a, the obtained kinetic swelling results do show the expected linearity of swelling versus time, at least in the later part of the kinetics, before a constant swelling at equilibrium is obtained. This suggests that Case II dominates the process of diffusion at 23 °C and the two-layer model is justified. For the higher temperature, 26 °C, the Case II front can be considered infinitely sharp, and the two-layer optical model holds very accurately. The higher temperature, however, causes relaxations to become much faster, and the diffusion process is completed within just a few min (about 9 min for ≈120 nm films). This makes accurate measurements more challenging, especially for thinner films, because the time spent for setting up

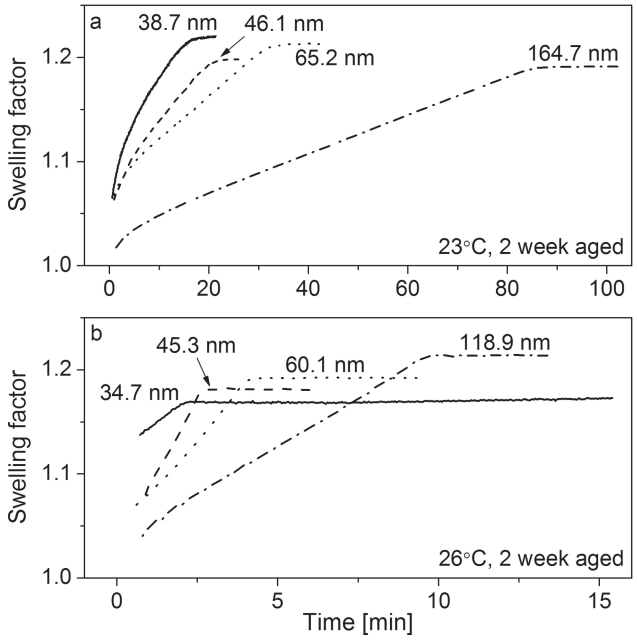

Figure 2. Kinetics of swelling, obtained with the two-layer optical model, for 23 °C (a) and 26 °C (b) for samples aged for 2 weeks, only 4 data series, out of 9 (a) or 10 (b) measured, are shown on each graph. The values at the curves correspond to dry film thicknesses.

of the experiment (<45 s) becomes more significant. The large effect of temperature is a result of a high activation energy of the chain relaxation process at the front, E_a = 241 kJ mol^{-1}.[45] Temperatures outside of the range 23–26 °C were considered not suitable for our measurements. Below 23 °C, the timescales of diffusion and chain relaxation start to overlap and the Case II character is lost, above 26 °C, the progression of the diffusion front is too fast to accurately resolve Case II kinetics for thinner films (<50 nm).

4.1. Ellipsometric Modeling of Dynamic Swelling

Swelling kinetics at 23 °C and 26 °C, for samples aged for 2 weeks, are presented in Figure 2. The swelling factor has been obtained using the two-layer optical model, and can be expressed by:

$$S_F(t) = \frac{h_{\text{swollen}}(t)\cdot S_{F,\text{eq.}} + \left(h_{\text{dry}} - h_{\text{swollen}}(t)\right)}{h_{\text{dry}}} = \frac{h_{\text{swollen}}(t)\cdot\left(S_{F,\text{eq.}} - 1\right)}{h_{\text{dry}}} + 1 \quad (3)$$

In this equation, h_{swollen} is the thickness of the part of the dry film that is replaced by a penetrant swollen layer of thickness $h_{\text{swollen}}\cdot S_{\text{F,eq}}$ (assuming relative dilation equal to that at equilibrium swelling of the entire film: $S_{\text{F,eq.}}$). The thickness of the layer that is not yet swollen is $h_{\text{dry}} - h_{\text{swollen}}$, with h_{dry} the initial thickness of the completely dry film.

All films presented in Figure 2 exhibit similar qualitative behavior; faster swelling at the beginning of the curve with a slight exponential character, followed by a linear increase in thickness. Similar observations have been made by Hori et al.[18] for methanol diffusion in PMMA. These authors have interpreted the faster initial swelling as faster diffusion through the outer interface of the thin film, suggesting that this outer interface has a region with different than bulk dynamics. Our results support a similar proposition for the n-hexane–polystyrene system. At the beginning, when the penetrant enters a thin film, its diffusion speed is higher than in a later stage in a bulk-like region. The initial fast swelling is observed consistently for all analyzed samples, at both swelling temperatures (23 °C and 26 °C), and at both aging histories (1 h and 2 weeks).

In particular, the results for the thinnest films (38.7 nm in Figure 2a and 34.7 nm in Figure 2b) suggest the presence of an interfacial layer that is swollen almost instantly at the beginning of the experiments. For these thinnest films, the swelling curves show a discontinuity in the initial stage.

To quantify the thickness of the instantly swollen interfacial layer, Figure 3 and 4 are presented. Figure 3 shows the swelling factor, $S_F(t)$, versus dry film thickness for two time slices, 1 min and 5 min, for nine thin film samples swollen at 23 °C aged for 2 weeks. For thinner films, the swelling factor is larger due to the relatively larger contribution of the swollen film to the overall film thickness at the same time slice (as a consequence of $S_F \sim 1/h_{\text{dry}}$). The lines in Figure 3 correspond to a numerical fit of

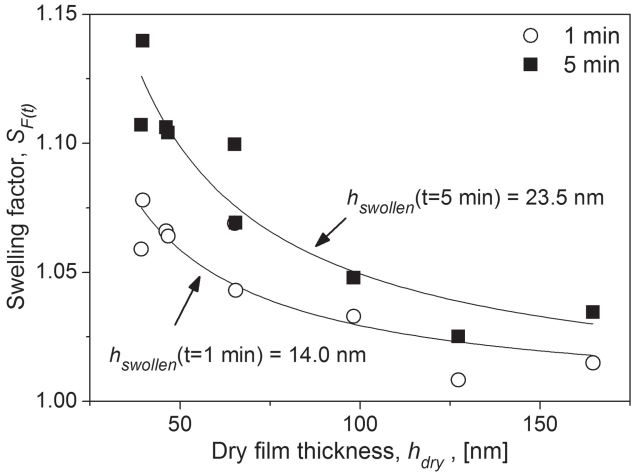

Figure 3. Swelling factor after 1 min and after 5 min as a function of a dry film thickness for 9 samples swollen at 23 °C aged for 2 weeks; solid line represents numerical fits of the Equation 3 assuming a two-layer mobility profile with h_{swollen} as a single fit parameter.

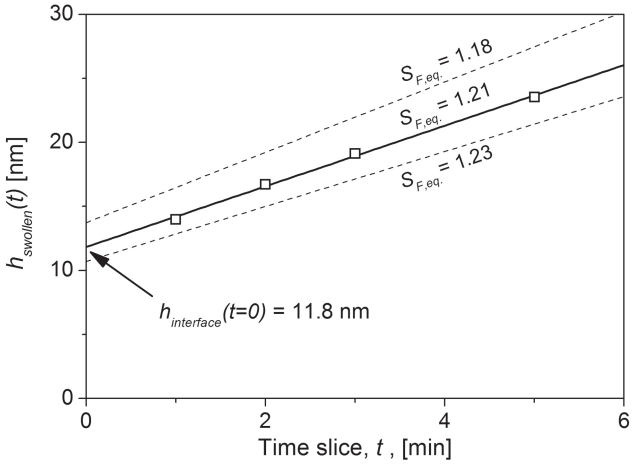

Figure 4. Interfacial swollen layer thickness, $h_{swollen}$, at several time slices for a series of nine thin films swollen at 23 °C aged for 2 weeks; intercept at t = 0 represents a region of the film swollen instantly.

Equation 3 to the swelling of all nine samples simultaneously, using only $h_{swollen}$ as fitting parameter, therefore extracting the swollen layer thickness at a given time slice. As value for $S_{F,eq.}$, the average swelling at equilibrium of all nine samples is taken. The value of $S_{F,eq.}$ is found to be within ±0.015 from the equilibrium swelling of thicker samples (>80 nm) where a more accurate determination of thickness and refractive index by ellipsometry is possible. This additional finding suggests no significant deviations of $S_{F,eq.}$ for the ultra-thin films. The simultaneous fit for all samples allows moderating the scatter in $h_{swollen}$ obtained for thinner films.

Fit values for $h_{swollen}(t)$ obtained at 23 °C for a series of nine samples aged for 2 weeks with $S_{F,eq.}$ = 1.21 are shown in Figure 4 as a function of the time of exposure to n-hexane. The solid line represents a linear fit through the data points. The slope of this line corresponds to the velocity of the front, moving in the direction perpendicular to the substrate interface. The linear behavior indicates that, during the time intervals in between 1 and 5 min (well after the penetration of the interface), the velocity of the front is independent of the position in the film. The numerical value of the front velocity is calculated to be ≈2.4 nm min^{-1}. The intercept corresponds to the thickness of an interfacial layer that is swollen instantly when the film comes in contact with n-hexane. The value of the thickness of this fast swelling layer is $h_{interface}(t = 0)$ = 11.8 ± 0.3 nm and corresponds to $h_{swollen}(t = 0)$. The extrapolation of the linear trend to t = 0 implies that swelling of the thin interface layer is assumed infinitely fast. The persistence of the linear trend (R^2 = 0.9975) to short experimental times (1 min) suggests that indeed a very significant difference in dynamic behavior between the outer polymer interface and the rest of the film exists. This is also in agreement with swelling curves shown in Figure 2. A similar description of ultra-thin polystyrene films supported on silicon substrates was found to be valid for polymer viscosity profiles, where evidence of very fast mobility layer at the outer film interface has been found.[24]

The dashed lines in Figure 4 demonstrate the sensitivity of the value of $h_{swollen}(t)$ and $h_{interface}(t = 0)$ for an experimental error in $S_{F,eq.}$. Results for the two most extreme values for $S_{F,eq.}$, obtained for the nine samples, are plotted. Similar results were obtained for the three remaining sets of samples and the resulting $h_{interface}(t = 0)$ values are presented in a comparative Figure 6 (combining results of sections 4.1. and 4.2.) as open symbols. The error bars represent the limits as demonstrated with dashed lines in Figure 4.

The quantification of the interfacial layer thickness, based on our modeling data, involves some assumptions. One assumption is that the effects of interactions between PS layer and the substrate are regarded negligible due to unfavorable interaction of the polymer and SiO_x surface of the wafer.[26] In contrast to PMMA supported on silicon wafers, for the PS significant immobilization of the polymer chains does not seem to occur.[24,26] Another assumption is that the interfacial layer is assumed to be swollen instantly upon contact with n-hexane, and that the swelling degree of the interfacial layers is identical to that of the bulk. This last assumption is based on the nonexistence of statistically significant deviations in equilibrium bulk swelling with decreasing film thickness. The equilibrium swelling of all analyzed films (7–10 films for each set) is within a range $S_{F,eq.}$ = 1.18–1.23 with no apparent trends with thickness. This rather broad obtained range of $S_{F,eq.}$ is also related to the inaccuracies inherent to the modeling of the ellipsometric data for very thin films (decoupling of thickness and refractive index).[41] Because of that, unfortunately, increased or decreased overall swelling of the thinner films could not be conclusively determined.

4.2. Kinetic Analysis of Raw Ψ and Δ Spectra

As an alternative to the model-dependent approach of the previous paragraph, it is possible to analyze dynamic evolution of raw Ψ and Δ parameters. This analysis is simplified by the fact that for pure Case II diffusion the front velocity is constant, which is manifested by a linear proportionality between the swelling and the time of exposure to the solvent. The duration for equilibration of the system (the time required for the front to travel through the entire film) is readily available from the raw spectra, from the instance after which no significant changes in the Ψ and Δ are observed. This instance can be extracted by finding the intersection of linear fits of either the Ψ

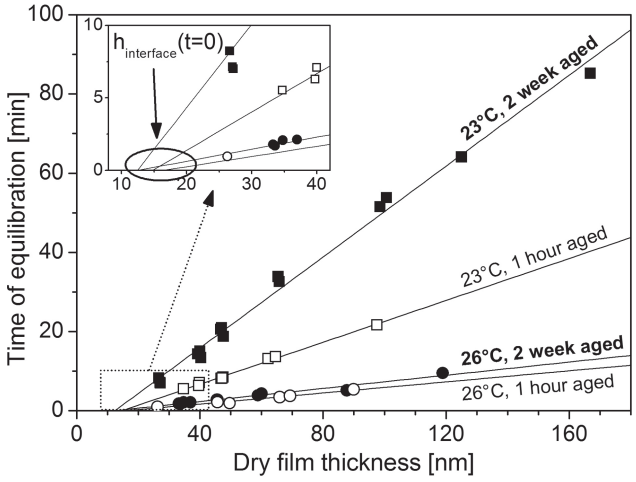

Figure 5. Time of equilibration as a function of dry polystyrene thin film thickness for all analyzed samples, inset shows a finite apparent film thickness at the time of equilibration = 0.

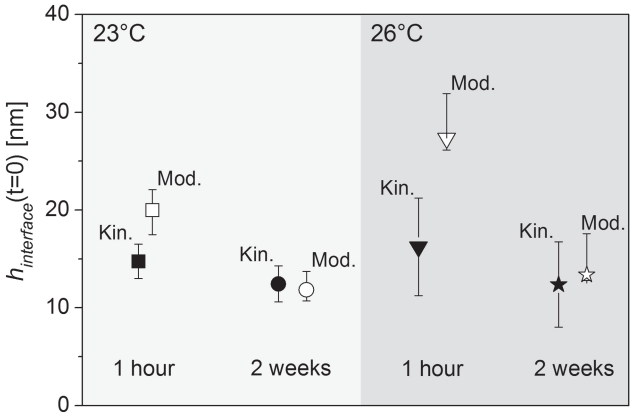

Figure 6. Thickness of the increased mobility layer obtained from modeling (Section 4.1) and kinetic analysis (Section 4.2) as a function of swelling temperature and aging time; for the kinetic data the error bars are calculated from combination of standard errors in slope and offset determination, for the modeling data, the error bars represent limits when extreme values of $S_{F,eq.}$ are taken (see Section 4.1.).

or Δ time evolution; one fit from the constant speed of swelling (bulk-like dynamics) and one fit from the equilibrated system. The results of this approach for all analyzed sample sets are presented in Figure 5.

From Figure 5, it is apparent that the swelling kinetics are strongly affected by the sample thermal history, in particular for the temperature close to the T_g. This is rationalized by the fact that the kinetics of Case II diffusion are dictated by chain relaxations. For aged samples, that are closer to their equilibrium state, n-hexane-induced chain relaxations are known to be slower.[39,45,47] For the experiments at 23 °C, close to the T_g, the chain dynamics are very slow and the effects of aging are amplified; the samples aged for 2 weeks require more than twice the time to equilibrate as compared with the samples aged for 1 h. For the 26 °C, further away from the T_g, the chain dynamics are much faster. The required equilibrium times at this temperature are much shorter as compared with the experiments at 23 °C, and the effects of aging are less pronounced. For all datasets, the data points can be fitted reasonably well using a simple linear fit (R^2 from 0.9628 to 0.9936). This is in agreement with the findings from Section 4.1., and implies that, after the interface is swollen, the front velocity shows no significant spatial variations in the direction perpendicular to the substrate. The constant front velocity allows accurate extrapolation of the time of equilibration for thinner films, from characterization of thicker films, at least in the range studied (up to about 165 nm), and possibly much further. This may have some practical utility, for instance, when knowledge of differences in diffusion timescales for different thicknesses of thin selective membranes is required.

All four linear fits do not go through the origin of the graph, but cross the *x*-axis at around 12–17 nm. The intersection point with the *x*-axis is shown more clearly in the inset of Figure 5. The *x*-intercept can be interpreted as the thickness of an interfacial region of the film that became swollen instantaneously within the time resolution of this experiment. Values for the thickness of such a layer, derived solely from the process kinetics, are in a reasonable agreement with the values obtained from the results of ellipsometric modeling presented in Section 4.1. The extracted *x*-axis intersection values for all datasets are collected in Figure 6 as closed symbols. The error bars are calculated from the combination of a standard error in the determination of the slope and offset of the linear fits.

4.3. Comparison of the Modeled and Kinetic Data Results

Figure 6 combines the values of $h_{interface}(t = 0)$ obtained from the modeling (Section 4.1.) and the kinetic analysis (Section 4.2.). The results obtained from the two distinct methods are in a reasonable agreement and seem to provide a strong evidence for different than bulk swelling behavior of the thin polystyrene film interface. The $h_{interface}(t = 0)$ is found to be, more or less, insensitive to the swelling temperature and the aging time. Higher error bars for the kinetic data for 26 °C are a result of larger error in determination of time of equilibration, due to much faster swelling of the samples swollen at this temperature. The obtained value of 27.4 nm for the modeling results (open triangle) is also larger than the smallest film thickness analyzed (26.8 nm), and therefore, has to be considered erroneous. This is probably an effect of the large impact of even small experimental errors on the results obtained

with ellipsometry modeling for ultra-thin films. In contrast, analysis of kinetic raw data, which avoids modeling issues, for that set of samples (closed triangle) yields a value for the interfacial film thickness that is in agreement with the results for the rest of the sample sets. The average $h_{interface}(t = 0)$ for all of the samples (excluding the modeling result for the 26 °C, 1 h aged sample), can be estimated at 14 ± 3 nm. This value is in a relatively good agreement with the reported range of increased polymer mobility for dry polymer systems (up to 10 nm).

The very fast swelling of the polymer interface can be arguably a manifestation of a few properties reported by other researchers. It can be assigned to much faster than bulk chain mobility of the polymer interface. In this case, the argument is that, since in Case II mechanism the front progression is related to local chain mobility, the interface mobility is much higher than in the rest of the film. On the other hand, the much faster swelling of the interface can be related to reduced viscosity (increased deformability and thus easier swelling) of the network at the interface.[32] Consistent with that interpretation, we find that the aging has no significant impact on the quantified thickness of the fast swollen layer (Figure 6).

The obtained thickness of the fast interface has been investigated here only for polystyrene of 280 kg mol^{-1} and n-hexane. Nano-confinement effects have been previously shown to weakly depend on the molecular weight of the polymer above a certain value.[48] This may also be the case for $h_{interface}(t = 0)$. Studies with lower molecular weight polystyrene, around the critical molecular weight for entanglements, can reveal the impact of the local inter- and intrachain entanglement density at the interfaces.

5. Conclusion

We have investigated the interfacial and bulk swelling kinetics of ultra-thin, silicon wafer supported, polystyrene films in liquid n-hexane in the temperature range where anomalous Case II diffusion is dominant. In this diffusion mechanism, a sharp front between the swollen and the non-swollen regions of a film develops and the progression velocity of this front depends on local polymer chain mobility. By means of time-resolved spectroscopic ellipsometry, spatial variations in the progression velocity can be determined in situ. Two distinct methods have been used for data interpretation. One method involves numerical fitting of a two-layer optical model to the ellipsometry spectra. The other method is based on monitoring of the time evolution of the raw ellipsometry data. For both methods, it is found that the diffusion of the liquid penetrant in the free surface of the film is much faster than the diffusion in the bulk, confirming the existence of a layer with significantly different than bulk properties at the ambient/film interface. The thickness of the fast interfacial region can be estimated to be 14 ± 3 nm, and does not depend on swelling temperature or physical aging time of the entire film. After the interface is swollen, the diffusion front velocity shows no significant spatial variations in the direction perpendicular to the substrate, but is strongly dependent on temperature and sample aging history. The obtained results are interpreted in terms of the increased polymer chain mobility or decreased viscosity at the surface of the polymer films. The experimental study presented here further strengthens the body of evidence indicating significantly different than bulk dynamics of the surfaces of glassy polymers and may be helpful in rationalizing outcomes of other studies found in the literature.

Acknowledgements: M.W. acknowledges support through the Alexander von Humboldt Foundation.

Received: May 23, 2013; Revised: July 19, 2013; Published online: August 9, 2013; DOI: 10.1002/macp.201300371

Keywords: in situ spectroscopic ellipsometry; nanolayers; ultra-thin glassy films; surfaces; swelling

[1] B. Frank, A. P. Gast, T. P. Russell, H. R. Brown, C. Hawker, *Macromolecules* **1996**, *29*, 6531.
[2] G. B. DeMaggio, W. E. Frieze, D. W. Gidley, M. Zhu, H. A. Hristov, A. F. Yee, *Phys. Rev. Lett.* **1997**, *78*, 1524.
[3] J. L. Keddie, R. A. L. Jones, R. A. Cory, *Faraday Discuss.* **1994**, *98*, 219.
[4] R. A. L. Jones, *Curr. Opin. Colloid Interface Sci.* **1999**, *4*, 153.
[5] P. G. de Gennes, *Eur. Phys. J. E: Soft Matter Biol. Phys.* **2000**, *2*, 201.
[6] R. S. Tate, D. S. Fryer, S. Paqualini, M. F. Montague, J. J. De Pablo, P. F. Nealey, *J. Chem. Phys.* **2001**, *115*, 9982.
[7] D. S. Fryer, P. F. Nealey, J. J. de Pablo, *Macromolecules* **2000**, *33*, 6439.
[8] J. A. Forrest, K. Dalnoki-Veress, *Adv. Colloid Interface Sci.* **2001**, *94*, 167.
[9] Z. Fakhraai, J. A. Forrest, *Science* **2008**, *319*, 600.
[10] Z. Fakhraai, J. A. Forrest, *Phys. Rev. Lett.* **2005**, *95*, 025701.
[11] S. Peter, H. Meyer, J. Baschnagel, *J. Polym. Sci., Part B: Polym. Phys.* **2006**, *44*, 2951.
[12] J. E. Pye, C. B. Roth, *Phys. Rev. Lett.* **2011**, *107*, 235701.
[13] J. E. Pye, K. A. Rohald, E. A. Baker, C. B. Roth, *Macromolecules* **2010**, *43*, 8296.
[14] C. Rotella, S. Napolitano, M. Wübbenhorst, *Macromolecules* **2009**, *42*, 1415.
[15] Z. Yang, Y. Fujii, F. K. Lee, C.-H. Lam, O. K. C. Tsui, *Science* **2010**, *328*, 1676.
[16] J. H. Kim, J. Jang, W.-C. Zin, *Langmuir.* **2001**, *17*, 2703.
[17] J. Q. Pham, S. M. Sirard, K. P. Johnston, P. F. Green, *Phys. Rev. Lett.* **2003**, *91*, 175503.
[18] K. Hori, H. Matsuno, K. Tanaka, *Soft Matter.* **2011**, *7*, 10319.
[19] M. Tress, M. Erber, E. U. Mapesa, H. Huth, J. Müller, A. Serghei, C. Schick, K. J. Eichhorn, B. Voit, F. Kremer, *Macromolecules* **2010**, *43*, 9937.

[20] M. Erber, M. Tress, E. U. Mapesa, A. Serghei, K.-J. Eichhorn, B. Voit, F. Kremer, *Macromolecules* **2010**, *43*, 7729.
[21] J. F. Stanzione III, K. E. Strawhecker, R. P. Wool, *J. Non-Crystalline Solids* **2011**, *357*, 311.
[22] R. P. Wool, A. Campanella, *J. Polym. Sci., Part B: Polym. Phys.* **2009**, *47*, 2578.
[23] D. Wong, C. A. Jalbert, P. A. V. O'Rourke-Muisener, J. T. Koberstein, *Macromolecules* **2012**, *45*, 7973.
[24] D.-D. Peng, R.-X. Li, C.-H. Lam, O. C. Tsui, *Chin. J. Polym. Sci.* **2012**, *31*, 12.
[25] D. Cangialosi, A. Alegria, J. Colmenero, *Phys. Rev. E* **2007**, *76*, 011514.
[26] K. Paeng, R. Richert, M. D. Ediger, *Soft Matter* **2012**, *8*, 819.
[27] J. Dutcher, M. Ediger, *Science* **2008**, *319*, 577.
[28] A. Sepúlveda, E. Leon-Gutierrez, M. Gonzalez-Silveira, C. Rodríguez-Tinoco, M. T. Clavaguera-Mora, J. Rodríguez-Viejo, *Phys. Rev. Lett.* **2011**, *107*, 025901.
[29] J. M. Rathfon, R. W. Cohn, A. J. Crosby, J. P. Rothstein, G. N. Tew, *Macromolecules* **2011**, *44*, 5436.
[30] F. Brochard Wyart, P. G. de Gennes, *Eur. Phys. J. E.* **2000**, *1*, 93.
[31] F. Dubourg, J. P. Aimé, S. Marsaudon, G. Couturier, R. Boisgard, *J. Phys.: Condensed Matter.* **2003**, *15*, 6167.
[32] S. Napolitano, C. Rotella, M. Wübbenhorst, *ACS Macro Lett.* **2012**, *1* 1189.
[33] A. Singh, M. Mukherjee, *Macromolecules* **2003**, *36*, 8728.
[34] N. L. Thomas, A. H. Windle, *Polymer* **1982**, *23*, 529.
[35] N. L. Thomas, A. H. Windle, *Polymer* **1981**, *22*, 627.
[36] M. Artsis, A. Chalykh, N. Khalturinskii, Y. V. Moiseev, G. Zaikov, *Eur. Polym. J.* **1972**, *8*, 613.
[37] C. J. Durning, M. M. Hassan, H. M. Tong, K. W. Lee, *Macromolecules* **1995**, *28*, 4234.
[38] M. Sanopoulou, D. F. Stamatialis, *Polymer* **2001**, *42*, 1429.
[39] L. Nicolais, E. Drioli, H. B. Hopfenberg, D. Tidone, *Polymer* **1977**, *18*, 1137.
[40] A. R. Berens, H. B. Hopfenberg, *Polymer* **1978**, *19*, 489.
[41] H. Fujiwara, I. Wiley, *Spectroscopic Ellipsometry Principles and Applications*, John Wiley & Sons, Chichester, England; Hoboken, NJ **2007**.
[42] H. G. Tompkins, E. A. Irene, *Handbook of Ellipsometry*, William Andrew Pub., Springer, Norwich, NY, USA; Heidelberg, Germany **2005**.
[43] L. Meli, J. Q. Pham, K. P. Johnston, P. F. Green, *Phys. Rev. E* **2004**, *69*, 051601.
[44] J. Q. Pham, K. P. Johnston, P. F. Green, *J. Phys. Chem. B.* **2004**, *108*, 3457.
[45] W. Ogieglo, H. Wormeester, M. Wessling, N. E. Benes, *Polymer* **2013**, *54*, 341.
[46] R. Stokes, *J. Chem. Thermodynamics* **1973**, *5*, 379.
[47] G. C. Sarti, A. Apicella, C. De Notaristefani, *J. Appl. Polym. Sci.* **1984**, *29*, 4145.
[48] O. K. C. Tsui, H. F. Zhang, *Macromolecules* **2001**, *34*, 9139.